# Effect of microwave heating duration on the stability of the partially stabilised zirconia doped with CaO

Qiannan Li [a, b], Yeqing Ling [a, b], Hewen Zheng [a, b], Mamdouh Omran [c], Kangqiang Li [b], Lei Gao [a, *], Mingyuan Zhang [a], Jin Chen [b, **], Guo Chen [a, b, **]

[a] *Kunming Key Laboratory of Energy Materials Chemistry, Key Laboratory of Green-Chemistry Materials in University of Yunnan Province, Yunnan Minzu University, Kunming 650500, PR China.*

[b] *Key Laboratory of Unconventional Metallurgy, Ministry of Education, Kunming University of Science and Technology, Kunming 650500, PR China.*

[c] *Faculty of Technology, University of Oulu, Finland.*

[*] Corresponding author: glkust2013@hotmail.com

[**] Co-corresponding author: guochen@kust@edu.cn, jinchen@kust.edu.cn.

**Abstract:**

In this paper, the stability of CaO doped partially stabilised zirconia (CaO-PSZ) prepared by electrofusion method was improved from 88.14% to 95% within one hour using the microwave heating method. The increase of the stability rate was because of the microwave heating method's advantages, including selective heating and fast heating. Analysis techniques, namely X-ray diffraction (XRD), Fourier transform infrared (FT-IR), Raman spectroscopy, and scanning electron microscopy (SEM), were used to analysis the influences of the holding time (1-4 h) on the CaO doped PSZ samples at a heating temperature of 1100 °C to understand the fundamental mechanism of the optimisation process. The Raman and XRD spectra were fitted by the Gaussian method to further analysis the effect of holding time on the microstructure evolution of the samples. The fitting results indicated that the sample's crystal quality and stability were improved after microwave heating, and the optimised holding time is 2h.

**Keywords:** microwave heating; holding time; zirconia; calcium oxide; stability

## 1. Introduction

Zirconia ($ZrO_2$) has inactivity chemical properties and unique physical properties i.e. high melting point, high resistivity, chemical corrosion resistance, and wear resistance [1-4]. Thus, the applications of $ZrO_2$ i.e. high-temperature resistant material, ceramic insulation material, and ceramic shading agent, are widely concerned in aspects including aerospace, large-scale thermal power generation, chemical industry, and metallurgy. Additionally, $ZrO_2$ has applications for improving the performances of high-temperature structural ceramics, electronic ceramics, and bio-ceramics.

At atmospheric pressure, there are three phases of pure zirconia with different structures, namely the monoclinic phase (m-$ZrO_2$), tetragonal phase (t-$ZrO_2$), and cubic phase (c-$ZrO_2$), among which m-$ZrO_2$ is the most common phase existed at room temperature [5-7]. During the heating or cooling process of pure zirconia, martensitic transformation appears at a temperature of 1170 ℃ with the transformation between the tetragonal phase and monoclinic phase, providing improved toughness of ceramic materials [8,9]. However, the 3% - 5% volume expansion/shrinkage occurs during martensitic transformation, leading to cracks in the microstructure of this potential material, and thus causes unstable thermal behaviour [7, 10-12].

Researchers addressed this problem and used doping as one of the key factors to control the stability of the $ZrO_2$ phase structure. Doping allows the cation of dopant to replace the position of $Zr^{4+}$, and thus forming a substitutional solid solution. There are mainly two kinds of stabilised zirconia prepared by doping stabilisers, i.e. fully stabilised zirconia (FSZ) and partially stabilised zirconia (PSZ). The fully stable zirconia is 100% cubic phase zirconia in

which a solid solution is formed. Thus, temperature change has few effects on the phase composition in the fully stable zirconia, making FSZ a material for thermocouple protection. However, FSZ has a high thermal expansion coefficient which limited the service life of FSZ as a structural material in the high-temperature environment. PSZ, formed by co-existed cubic phase and part of the tetragonal phase, shows a better thermal performance than FSZ, thus attached more attention in the industrial applications with pyro-process.

The commonly used dopants for the preparation of partially stabilised zirconia include CaO, MgO, $Y_2O_3$, and $Ce_2O_3$ [13-18]. MgO-PSZ is a famous material in the modern ceramic family. It has an application in the oxygen sensor for monitoring oxygen activity in molten steel. However, MgO-PSZ is prone to decompose at a temperature above 1000 °C, which limits its application in a high-temperature region. Recently, researchers have focused on yttria partially stabilised zirconia, which has good mechanical properties, strong toughness, and good heating properties. Sun et al. prepared yttrium oxide partially stabilised zirconia (YSZ) nano-coating materials by atmospheric plasma spraying (APS), indicating that the prepared nanostructured coating material has long thermal cycle life and good thermal cycling oxidation performance [19]. However, the high cost and the low-temperature ageing of YSZ limited the application of this potential material. Thus, calcium-stabilised zirconia with advantages i.e. low cost, high ionic conductivity, low thermal conductivity, and excellent thermal shock resistance, has received attention in the applications in oxygen sensors and high-temperature heaters.

At present, electrofusion is the main approach for the mentioned zirconia materials. Electrofusion is a simple process with advantages, including a short procedure and low

product cost. However, the method also suffers from disadvantages, including low stability of the produced samples, high heat treatment temperature, and the corresponding high energy consumption [20,21]. Therefore, a preparation method for optimizing the stability of partially stabilised zirconia samples with a short operation time is required. Among the preparation methods for PSZ, microwave heating has attracted the attention of researchers. With microwave heating, the reactant molecules' internal structure will oscillate and thus generate energy for heating [22,23]. Compared with electrofusion, microwave heating has the advantages of selective heating, rapid heating, energy-saving, and high efficiency [24,25]. Also, microwave heating can control the crystal form and affects the stability of partially stabilised zirconia [26,27]. Li et al. prepared calcium oxide partially stabilised zirconia (CaO-PSZ) by microwave heating method [28]. The results show that calcium oxide partially stabilised zirconia was formed from molten zirconia using microwave heating at a temperature of 1450 °C for two hours, and CaO stabiliser precipitated at the grain boundary, forming needle-like grains and fine particles, which enhanced the toughness of CaO-PSZ. Therefore, more and more researchers choose to use microwave heating technology to prepare partially stable zirconia. Guo et al. prepared partially stabilised zirconia by microwave roasting. The results show that a better crystal form and a better microstructure of the partially stable zirconia appeared at a calcination temperature of 1723 K and a holding time of 240 min [29]. Khollam et al. prepared yttrium stabilised cubic zirconia materials by microwave hydrothermal synthesis method presented energy-saving characteristics and improved thermal stability of the products [30].

In this experiment, for optimisation of the stability of CaO doped partially stabilised zirconia, we using microwave heating with a heating temperature of 1100 °C. The influence of holding time (1-4 h) on the stability of CaO doped partially stabilised zirconia was analysed. The details for the mechanism of phase transformation were studied. The purpose is to provide more practical cases for the development of microwave heating in the preparation of CaO-PSZ materials.

## 2. Experiment

### *2.1 Materials*

The raw material of zirconia used in this project is from Zhengzhou (Henan Province, China), produced by electric arc process. Other chemical reagents used in this study are of analytical grade without further purification. The main chemical composition of zirconia is shown in Table 1, indicating that the main component of zirconia is 94.85% of $ZrO_2$, 0.4% of $Al_2O_3$, 0.4% of $SiO_2$, 0.2% of $TiO_2$, 0.15% of $Fe_2O_3$, and 4% of CaO as a stabilizer, suggesting that $ZrO_2$ and CaO phases are the main components of fused zirconia. The XRD diagram of the zirconia sample and the corresponding analysis were described in Fig. 1.

According to the standard card of cubic zirconia (c-$ZrO_2$, JCPDS: 49-1642), monoclinic zirconia (m-$ZrO_2$, JCPDS: 37-1484), and tetragonal zirconia (t-$ZrO_2$, JCPDS: 42-1164), monoclinic zirconia and cubic zirconia exist in the zirconia samples, and the diffraction peak of tetragonal zirconia overlaps with the diffraction peak of cubic zirconia. Thus, the evidence for the existence of the tetragonal phase in zirconia raw materials is insufficient. Also, the diffraction peak of CaO phase is absent in the diagram, which indicates that CaO has entered

the lattice node of $ZrO_2$ and formed a stable replacement solid solution structure with zirconia ($ZrO_2$). In conclusion, the as-received zirconia samples belong to CaO-PSZ ceramic materials.

### *2.2 Equipment*

In this experiment, the microwave heating method was used. The microwave frequency of the muffle furnace used in this experiment was 2.45 GHz, and the microwave output power was controllable (0-1.5 kW). Fig. 2 shows the schematic diagram of the microwave calcining equipment, mainly composed of a circulating water-cooling system, microwave heating system, sample box, and temperature control system.

### *2.3 Experimental procedure*

In this experiment, fused zirconia stabilised by CaO was put into a drying oven (FX101-1) and dried at 105 °C for 12 h. Then, the dried samples were compacted and subsequently put into a horizontal microwave reactor and calcined for 60 min under the conditions of a microwave output power of 3 kW and a calcination temperature of 1100 °C. A temperature control system was responsible for keeping the heating rate constant at 8 ℃/min. During the heating process, the sample temperature was detected by an infrared thermometer, and the temperature measurement accuracy was ±2 °C. After calcination, the sample was naturally cooling to room temperature. Then 40 g of the sample was divided into four equal parts, and the effect of holding time on the stability of partially stabilised zirconia was tested. In this experiment, the calcination temperature was 1100 °C, and the calcination holding time was 1 h, 2 h, 3 h, and 4 h, respectively. After the holding time reached the settled value, the microwave heating was turned off, and the samples were naturally cooled to room temperature to extract the calcined products for further analysis.

### *2.4 Characterization*

The phase analysis of the heated products was carried out by X-ray diffraction (D8 advance a25×). The target source was copper target Kα ray (λ=0.154056 nm), tube voltage and current are 40 kV and 20 mA, scanning range was 0 °~100 °, scanning speed was 5 °/min. Raman spectroscopy (Renishaw Raman scope system 1000) was used to analyse the molecular vibration information of the heated products, and the molecular structure of the heated products was studied. Fourier transform infrared (IS10, Nicolet, USA) was used to analyse the surface functional groups and their chemical structures of the calcined products. The spectral range was 4000-500 $cm^{-1}$. The microstructure of calcined products was determined by FESEM (XL30ESEM-TMP, Philips, Holland) with an accelerating voltage of 30 kV. In this project, all measurements were carried out at room temperature.

## 3. Results and discussion

### *3.1 Characterization by XRD*

The crystal structures of the CaO-PSZ samples calcined for 1 h, 2 h, 3 h, and 4 h were characterised by XRD, respectively. In Fig. 3, XRD results indicate that the phase composition of CaO-PSZ samples heated by microwave was a mixed phase. Limited diffraction peaks for monoclinic zirconia appear at 2θ=28.214 ° and diffraction peaks for cubic zirconia appear at 2θ=30.177 °, 2θ=59.777 °, and 2θ=81.766 °, respectively. Because the diffraction peaks appear at 2θ=34.897 ° and 2θ=50.174 ° are both characteristic peaks for tetragonal zirconia and cubic zirconia, we suspect that tetragonal zirconia was transformed from monoclinic zirconia. The evidence to support this is that the characteristic peaks of

monoclinic zirconia were reduced in all the XRD patterns of the prepared samples compared to the as-received sample.

The trajectories of the characteristic peaks of the cubic, tetragonal and monoclinic phases were fitted by Gaussian mathematical model to understand the effect of microwave heating duration on the samples, as shown in Figs. 4(a) - (e). The results show that the half-width of the main peak of monoclinic zirconia was 0.284, 0.281, 0.398, and 0.477, respectively, and that of cubic phase was 0.175, 0.160, 0.166, and 0.168 at the conditions with a holding time of 1 h, 2 h, 3 h, and 4 h, respectively. Compared with the samples received (the half peak width of monoclinic zirconia peak is 0.454, and that of cubic phase zirconia is 0.274), the crystallinity of the sample was improved by extending the holding time, and the best crystallinity of the sample was achieved when the holding time was 2 h. According to the fitting results, the grain half peak width becomes smaller after microwave heating, which indicates that the grains are aggregated and grown-up.

The relative monoclinic content ($V_m$) was measured by XRD analysis to evaluate the relative ratio of monoclinic zirconia to the summary of monoclinic and cubic phases, and calculated according to the equation proposed by Garvie et al.[31] and modified by Toraya et al.[32]:

$$V_m = \frac{1.311[I_m(\bar{1}11)+I_m(111)]}{1.311[I_m(\bar{1}11)+I_m(111)]+I_c(111)} \quad (1)$$

where $I_m$ and $I_c$ are the intensity of the monoclinic and cubic peaks, respectively. The monoclinic phase and cubic phase's relative contents for the original sample and the sample with a holding time of 1 h, 2 h, 3 h, and 4 h were plotted as shown in Figure 5. It can be seen from Figure 5 that with the prolongation of the holding time, the relative content of the cubic

phase increases and reaches the highest value (94.46%) at 2 h. In comparison, the monoclinic phase's relative content decreases and reaches the lowest value (5.54%) at 2 h. After 2 hours of microwave heating, the monoclinic phase increased with the further prolongation of the holding time, which is unwelcome by forming high-quality samples.

### *3.2 Characterization by Raman spectroscopy*

Figs. 6(a)-(b) present the Raman spectrums of zirconia obtained from the Raman scattering digital image collected in the spectral scattering detection area from 100 $cm^{-1}$ to 650 $cm^{-1}$. The change of Raman vibration characteristic peak can further confirm the existence of the tetragonal phase in zirconia. Fig. 6(a) exhibits that five kinds of Raman activities appear in the Raman spectra of CaO-PSZ. The two peaks at 286.8 $cm^{-1}$ and 316.0 $cm^{-1}$ results from the $E_g$ and $B_{1g}$ Raman vibrations of tetragonal zirconia. The three peaks at 350.7 $cm^{-1}$, 374.6 $cm^{-1,}$ and 403.8 $cm^{-1}$ are the characteristic peaks of $B_g$ Raman vibration of monoclinic zirconia.

Differences in the test parameters and test conditions can cause significant differences in the signal strength. For a more scientific comparison, the data are usually normalised using the peak value. In this paper, the Raman spectra data of raw materials in Fig. 6(b) at 1 h, 2 h, 3 h, and 4 h are divided by the values of their strongest peaks, producing the normalised peak intensities in the range of 0-1. The results are shown in Fig. 6(b) with the calculation following Eq. (2):

$$Normalized\ intensity = \frac{Intensities\ of\ peak\ splitting}{Intensity\ of\ the\ strongest\ peak} \quad (2)$$

Fig. 6(b) reveals that there are five Raman activities at 403.5 $cm^{-1}$, 374.8 $cm^{-1}$, 350.7 $cm^{-1}$, 316.0 $cm^{-1}$ and 285.8 $cm^{-1}$, respectively. In Fig. 6(b), the characteristic peak of CaO is

absent for observing, which indicates that $CaO\text{-}ZrO_2$ is a complex mixed oxide. With the increase of holding time from 1 h to 4 h, a monoclinic peak (Raman shift = 350.7 $cm^{-1}$) with weak intensity appeared, and then the intensity slightly increased. Comparing the spectra of raw materials in Fig. 6(a) and that of the sample treated with microwave for 1 h in Fig. 6(b), the tetragonal phase's characteristic peaks became sharper. The characteristic peak of the monoclinic phase (Raman shift = 350.7 $cm^{-1}$) disappears, which indicates that the monoclinic phase has changed into the tetragonal phase.

To further understand the effect of microwave treatment on the phase composition of the samples, the trajectories of the vibration characteristic peaks of the tetragonal and monoclinic phases were fitted by the Gaussian mathematical model, as shown in Figs. 7(a)-(e).

Figs. 7(a)-(e) corresponds to the fitting curves of Raman spectra of raw materials and a holding time of 1 h, 2 h, 3 h, and 4 h, respectively. There are five characteristic peaks in the figures. Peaks (1) and (2) are characteristic peaks of the tetragonal phase, and peak (3), peak (4), and peak (5) are characteristic peaks of the monoclinic phase. In Figs. 7(a)-(e), the half-height width for characteristic peaks of the tetragonal phase is focused. To the raw material and the sample prepared with a holding time of 1 h, 2 h, 3 h, and 4 h, the corresponding value is 32.53, 29.54, 28.46, 24.72, and 27.43 for peak (1), respectively. The corresponding value for peak (2) is 12.39, 14.42, 13.34, 17.24, and 15.71, respectively. In the studied range of the microwave heating time, the samples' half-height width changed significantly after microwave treatment compared with the raw materials. It is also known that crystallinity has a negative relation with the half-height width. Peak (1) and peak (2) are

characteristic peaks of the tetragonal phase, the FWHM variation of which indicating that the crystallinity of the tetragonal phase is improved.

Additionally, the Area IntgP values are calculated by the relative percentage of the monoclinic/tetragonal phase's peak area to the total area of characteristic peaks of monoclinic and tetragonal phases understand the relative percentage content of the monoclinic/tetragonal phase. The results for the as-received sample and a holding time of 1h, 2h, 3h, and 4h are shown in Figs. 7(a)-(e), indicating that the Area IntgP values of tetragonal phase are 21.34, 21.89, 22.26, 20.15, and 21.52, respectively, the Area IntgP values of monoclinic phase are 78.65, 78.11, 77.74, 79.85, and 78.47, respectively. By analysing the Area IntgP values of the tetragonal phase and monoclinic phase, the holding time of 2 h caused the maximum Area IntgP value of the tetragonal phase and the minimum value of the monoclinic phase. According to the analysis of the half-width and the Area IntgP of the tetragonal phase, the optimum reaction conditions were obtained when the calcination temperature was 1100 °C with a holding time was 2 h, which was consistent with the XRD analysis results.

### *3.3 Characterization by FT-IR*

In this test, the surface functional groups of CaO-PSZ were analysed by scanning in the spectral scanning range of 4000-500 $cm^{-1}$, and the infrared spectral analysis is shown in Figs. 8(a)-(b).

Fig. 8(a) indicates five characteristic peaks in the infrared spectrum of fused zirconia stabilised by calcium oxide. Among them, the absorption peak at 1013.89 $cm^{-1}$ is an effect of the bending vibration of the O-H bond, the characteristic absorption peak at 1384.87 $cm^{-1}$ results from the sample adsorbing $CO_2$ in the air, the absorption peak at 1641.74 $cm^{-1}$ results

from the bending vibration of H-O-H on the sample surface, and the characteristic absorption peak at 3443.14 $cm^{-1}$ is resulted from the contraction vibration of O-H bond on the sample surface. The characteristic peak at 546.40 $cm^{-1}$ is the vibration frequency of metal-oxygen.

Fig. 8(b) exposes five characteristic peaks in the infrared spectrum of the CaO-PSZ sample at 1100 °C and a holding time of 1 h. Five characteristic peaks were noticed at 546.43 $cm^{-1}$, 1015.13 $cm^{-1}$, 1417.08 $cm^{-1}$, 1642.72 $cm^{-1,}$ and 3447.14 $cm^{-1}$, representing the stretching vibration of Zr-O bond, O-H bond, $CO_2$ in air, H-O-H bond on the sample surface, and O-H bond on the sample surface, respectively. Combined with the infrared spectrum analysis of holding time of 2 h, 3 h, and 4 h, the characteristic peak at 546.43 $cm^{-1}$ moves to a higher wavenumber with the increase of holding time, resulting in a blue shift. The blue shift was attributed to the continuous transformation process from m-$ZrO_2$ to t-$ZrO_2$, which increased the content of t-$ZrO_2$ in heated CaO-PSZ samples. The martensitic transformation at the heating temperature is mainly m-$ZrO_2$ to t-$ZrO_2$, and a part of t-$ZrO_2$ is transformed into c-$ZrO_2$, which further improves the phase stability of CaO-PSZ.

### *3.4 Characterisation by SEM*

The SEM images of PSZ under different holding times of 1 h, 2 h, 3 h, and 4 h with a holding temperature of 1100 ℃ are shown in Figs. 9(a)-(d), respectively. Fig. 9 presents that when the holding time is 1 h (Fig. 9(a)), the particle shape is irregular, and the sample's surface is coarse. The irregularity of particle shape is improved when the holding time is 2 h (Fig. 9(b)), and several cracks can be observed in the surface of the sample compared with that of holding for 1 h. The sample's surface becomes smoother when the holding time continues to increase to 3 h (Fig. 9(c)). Combined with XRD analysis, it can be seen that the

surface of the sample becomes smooth due to the phenomenon of grain growth. When the holding time is 4 h (Fig. 9(d)), the sample's surface is smooth, and the microstructure of the sample is more regular, which indicates that the extension of holding time promotes the fusion of grains in CaO-$ZrO_2$ ceramics.

### *3.5 Phase stability analysis*

The influences of different holding time on the stability of the sample at 1100 °C was studied. The calculation of the stability rate can measure the stability degree of the prepared zirconia. The "K value semi-quantitative method" is used to calculate the stability rate of the prepared partially stable zirconia. The calculation formula is as follows:

$$Index\ of\ stability = \frac{Intensity\ of\ 29.92^\circ}{Intensity\ of\ 28.06^\circ + Intensity\ of\ 31.24^\circ + Intensity\ of\ 29.92^\circ} \times 100\% \quad (3)$$

where the intensity of 29.92 °-the peak intensity of c-$ZrO_2$； intensity of 28.06 °, intensity of 31.24 °-the peak intensity of m-$ZrO_2$. The results in Fig. 10 indicating that the stability rate of zirconia stabilised by calcium oxide is 88.14%, and the stability rate of samples with a holding time of 1 h, 2 h, 3 h, and 4 h is 95.17%, 95.71%, 95.17%, and 95.21%, respectively.

Fig. 10 exhibits that with the increase of holding time, the stability rate of the prepared PSZ gradually increases and tends to be stable. The stability rate calculation shows that under the same temperature, the prolongation of the holding time increases the phase transition of the PSZ, which makes the stability rate fluctuate. This phenomenon is mainly due to the prolongation of holding time. A part of the monoclinic phase changes into the tetragonal phase, which leads to the decrease of monoclinic phase content. Because of the difference between the radius of $Ca^{2+}$ and $Zr^{4+}$, when $Ca^{2+}$ ions enter the $ZrO_2$ lattice and replace $Zr^{4+}$,

lattice distortion and micro stress will occur. This micro stress plays a role in restraining the transformation from t-$ZrO_2$ to m-$ZrO_2$.

On the other hand, the tetragonal phase transformed into the cubic phase at a temperature below the initial phase transition temperature (2370 °C for pure $ZrO_2$) [33,34]. The reason is that the $Ca^{2+}$ of the tetragonal phase will continuously accumulate to the grain surface during the heating process, and these $Ca^{2+}$ rich regions may gradually form the cubic phase. This phenomenon was noticed by Li et al. in their study related to CaO doped partially stabilised zirconia, and the phase transition temperature for c-$ZrO_2$ was 1100 °C [35]. Thus, the mentioned transformation mechanism was doubted to be responsible for the noticed c-$ZrO_2$ transformation in the present work. With the increase of holding time, the growth of some cubic zirconia grains was promoted under the mentioned transformation mechanism. Thus, the stability rate of partially stabilised zirconia was improved. With the further extension of holding time above 3 h, the crystal transformation of zirconia has an ignorable change, where the stability rate of partially stabilised zirconia was basically in equilibrium.

## 4. Conclusions

In this paper, the effects of different holding times on the phase transformation of partially stabilised zirconia were studied by analysing and characterising the experimental samples and controlling the holding temperature. The following conclusions were drawn:

(1) With the recommended microwave heating approach (at a heating temperature of 1100 °C for more than1h), the stability rate of the CaO doped $ZrO_2$ increased from 88.14% (original sample prepared by electrofusion) to above 95%.

(2) To understand the phase transformation phenomenon during the heating process, the Raman spectrum analysis of CaO doped PSZ heated at 1100 °C was presented. The half-height width of characteristic peaks and the corresponding IntgP values, namely the percentage of the peak area of monoclinic/tetragonal phase to the total area of characteristic peaks of monoclinic and tetragonal phases, were calculated, indicating that the peak of IntgP value of tetragonal phase and the valley value of monoclinic phase were achieved when holding time was 2 h.

(3) The c-$ZrO_2$ phase transformation temperature of the CaO doped PSZ (1100 °C) was noticed to be lower than that of pure $ZrO_2$ (2370 °C). The reason is that the $Ca^{2+}$ of the tetragonal phase will continuously accumulate to the grain surface during the heating process, and these $Ca^{2+}$ rich regions may gradually form the cubic phase.

**Acknowledgements**

Financial supports from the National Natural Science Foundation of China (No: 51764052) and Innovative Research Team (in Science and Technology) at University of Yunnan Province were sincerely acknowledged.

**References**

[1] J. Ouyang, Z. Zhou, H. L. Lun, Y. L. Xie, H. M. Yang, Thermal and Chemical Properties of Zirconia ($ZrO_2$) and Their Applications, Mater. China. 33 (6) (2014) 365-375. https://doi.org/10.7502/j.issn.1674-3962.2014.06.08.

[2] G. Chen, Y. Q. Ling, Q. N. Li, H. W. Zheng, K. Q. Li, Q. Jiang, J. Chen, M. Omran, L. Gao, Crystal structure and thermomechanical properties of CaO-PSZ ceramics synthesised

from fused $ZrO_2$, Ceram. Int. 46 (10) (2020) 15357-15363. https://doi.org/10.1016/j.ceramint.2020.03.079.

[3] M. Sabzi, S. M. Dezfuli, Z. Balak, Crystalline texture evolution, control of the tribocorrosion behavior, and significant enhancement of the abrasion properties of a Ni-P nanocomposite coating enhanced by zirconia nanoparticles, Int. J. Min. Met. Mater. 26 (8) (2019) 1020-1030. https://doi.org/10.1007/s12613-019-1805-x.

[4] F. Kazemi, F. Arianpour, M. Taheri, A. Saberi, H. R. Rezaie, Effects of chelating agent on sol-gel synthesis of nano zirconia: The comparison of Pechini and sugar-based methods, Int. J. Min. Met. Mater. 27 (5) 2019. https://doi.org/10.1007/s12613-019-1933-3.

[5] J. H. Pee, T. Akao, S. Ohtsuka, M. Hayakawa, The Kinetics of Isothermal Martensitic Transformation of Zirconia Containing a Small Amount of Yttria, Mater. Trans. 44 (9) (2003) 1783-1789. https://doi.org/10.2320/matertrans.44.1783.

[6] M. Hayakawa, J. H. Pee, Y. Fujiwara, Low temperature martensitic transformation of zirconia with low contents of yttria, J. Phys. IV. 112 (2003) 1103-1106. https://doi.org/10.1051/jp4:20031075.

[7] L. X. Ding, L. Wang, M. Nagashima, M. Hayakawa, A Dilatometric Study of the Martensitic Transformation of Zirconia Containing 1.8~2.0 mol% Yttria, Mater. Trans. 42 (3) (2001) 450-452. https://doi.org/10.2320/matertrans.42.450.

[8] W. C. J. Wei, Y. P. Lin, Mechanical and thermal shock properties of size graded MgO–PSZ refractory, J. Eur. Ceram. Soc. 20 (8) (2000) 1159-1167. https://doi.org/10.1016/S0955-2219(99)00243-5.

[9] G. Chen, Y. Q. Ling, Q. N. Li, H. W. Zheng, J. Chen, Stability properties and structural characteristics of CaO-partially stabilised zirconia ceramics synthesized from fused $ZrO_2$ by microwave heating, Ceram. Int. 46 (10) (2020) 16842-16848. https://doi.org/10.1016/j.ceramint.2020.03.261.

[10] P. M. Kelly, L. R. F. Rose, The martensitic transformation in ceramics — its role in transformation toughening, Prog. Mater. Sci. 47 (2002) 463-557. https://doi.org/10.1016/S0079-6425(00)00005-0.

[11] M. Hayakawa, Y. Inoue, M. Oka, H. Nakagawa, Martensitic Transformation and Mechanical Properties of (Y, Ce)-Tetragonal Zirconia Polycrystals, Mater. Trans., JIM. 36 (6) (1995) 729-734. https://doi.org/10.2320/matertrans1989.36.729.

[12] X. Y. Chen, X. H. Zheng, H. S. Fang, H. Z. Shi, X.F. Wang, H. M. Chen, The study of martensitic transformation and nanoscale surface relief in zirconia, J. Mater. Sci. Lett. 21 (5) (2002) 415-418. https://doi.org/10.1023/A:1014936007488.

[13] K. Q. Li, J. Chen, J. H. Peng, S. Koppala, G. Chen, One-step preparation of CaO-doped partially stabilised zirconia from fused zirconia, Ceram. Int. 46 (5) (2019). https://doi.org/10.1016/j.ceramint.2019.11.129.

[14] M. Y. Zhang, L. Gao, J. X. Kang, J. Pu, J. H. Peng, M. Omran, G. Chen, Stability optimisation of CaO-doped partially stabilised zirconia by microwave heating, Ceram. Int. 45(17) (2019) 23278-23282. https://doi.org/10.1016/j.ceramint.2019.08.024.

[15] G. Chen, Q. N. Li, Y. Q. Ling, H. W. Zheng, J. Chen, Q. Jiang, K. Q. Li, J. H. Peng, M. Omran, L. Gao, Phase stability and microstructure morphology of microwave -sintered magnesia-partially stabilised zirconia, Ceram. Int. 2020. https://doi.org/10.1016/j.ceramint.2020.09.281.

[16] Y. Q. Ling, Q. N. Li, H. W. Zheng, M. Omran, L. Gao, J. Chen, G. Chen, Optimisation on the stability of CaO-doped partially stabilised zirconia by microwave heating, Ceram. Int. 2020. https://doi.org/10.1016/ j.ceramint.2020.11.161.

[17] K. Q. Li, Q. Jiang, G. Chen, L. Gao, J. H. Peng, Q. Chen, S. Koppala, M. Omran, J. Chen,

Kinetics characteristics and microwave reduction behavior of walnut shell-pyrolusite blends, Bioresour. Technol. 2021. https://doi.org/10.1016/j.biortech.2020.124172.

[18] D. P. Zhan, Effects of yttrium and zirconium additions on inclusions and mechanical properties of a reduced activation ferritic/martensitic steel, J. Iron. Steel. Res. Int. 2019. https://doi.org/ 10.1007/s42243-019-00332-9.

[19] J. Sun, L. L. Zhang, D. Zhao, Microstructure and thermal cycling behaviour of nanostructured yttria partially stabilised zirconia (YSZ) thermal barrier coatings, J. Rare Earths. 28 (S1) (2010) 198-201. https://doi.org/10.1016/s1002-0721(10)60302-x.

[20] P. Dahl, I. Kaus, Z. Zhao, M. Johnsson, M. Nygren, K. Wiik, T. Grande, M. A. Einarsrud, Densification and properties of zirconia prepared by three different heating techniques, Ceram. Int. 33 (8) (2007) 1603-1610. https://doi.org/10.1016/j.ceramint.2006.07.005.

[21] A. P. Singh, N. Kaur, A. Kumar, K. L. Singh, Preparation of Fully Cubic Calcium-Stabilised Zirconia With 10 mol% Calcium Oxide Dopant Concentration by Microwave Processing, J. Am. Ceram. Soc. 90 (3) (2010) 789-796. https://doi.org/10.1111/j.1551-2916.2006.01379.x.

[22] L. J. Liu, D. B. Li, J. H. Peng, S. H. Guo, L. B. Zhang, G. Chen, Preparation of Partially Stabilised Zirconia by Microwave Heating and Study on Prediction of the Stability, Mater. Rev. 25 (2011) 131-134. https://doi.org/10.1097/TA.0b013e3181f31e37.

[23] J. Li, J. H. Peng, S. H. Guo, L. B. Zhang, Preparation of Zirconia Ceramics Stabilised Partially by Microwave Heating Natural Baddeleyite, Titanium Ing. Prog. 3 (2011) 14-16. https://doi.org/10.13567/j.cnki.issn1009-9964.2011.03.012. (in Chinese)

[24] K. Q. Li, Q. Jiang, J. Chen, J. H. Peng, G. Chen, The controlled preparation and stability mechanism of partially stabilised zirconia by microwave intensification, Ceram. Int. 46 (6)

(2019). https://doi.org/10.1016/j.ceramint.2019.11.251.

[25] B. Makuza, Q. Tian, X. Guo, K. Chattopadhyay, D. Yu, Pyrometallurgical options for recycling spent lithium-ion batteries: A comprehensive review, J. Power. Sources. 491 (2021) 229622. https://doi.org/10.1016/j.jpowsour.2021.229622.

[26] G. Chen, K. Q. Li, Q. Jiang, X. P. Li, J. H. Peng, M. Omran, J. Chen, Microstructure and enhanced volume density properties of FeMn78C8.0 alloy prepared via a cleaner microwave heating approach, J. Clean. Prod. 262 (2020) 121364. https://doi.org/10.1016/j.jclepro.2020.121364.

[27] K. Q. Li, J. Chen, J. H. Peng, R. Ruan, C. Srinivasakannan, G. Chen, Pilot-scale study on enhanced carbothermal reduction of low-grade pyrolusite using microwave heating, Powder. Technol. 360 (2020) 846-854. https://doi.org/10.1016/j.powtec.2019.11.015.

[28] K. Q. Li, Q. Jiang, J. Chen, J. H. Peng, X. P. Li, S. Koppala, M. Omran, G. Chen, The controlled preparation and stability mechanism of partially stabilised zirconia by microwave intensification, Ceram. Int. 46 (6) (2020). https://doi.org/10.1016/j.ceramint.2019.11.251.

[29] S. H. Guo, G. Chen, J. H. Peng, J. Chen, J. L. Mao, D. B. Li, L. J. Liu, Preparation of partially stabilised zirconia from fused zirconia using roasting, J. Alloys Compd. 506 (1) (2010) L5-L7. https://doi.org/10.1016/j.jallcom.2010.06.156.

[30] Y. B. Khollam, A. S. Deshpande, A. J. Patil, H. S. Potdar, S. B. Deshpande, S. K. Date, Synthesis of yttria stabilised cubic zirconia (YSZ) powders by microwave-hydrothermal route, Mater. Chem. Phys. 71 (3) (2001) 235-241. https://doi.org/10.1016/S0254-0584(01)00287-5.

[31] R. C. Garvie, P. S. Nicholson, Phase analysis in zirconia systems, J. Am. Ceram. Soc. 55 (6) (1972) 303-305. https://doi.org/10.1111/j.1151-2916.1972.tb11290.x.

[32] H. Toraya, M. Yoshimura, S. S. Somiya, Calibration curve for quantitative analysis of the

monoclinic-tetragonal Zr02 system by X-Ray diffraction, J. Am. Ceram. Soc. 67 (June) (1984) C119-C121. https://doi.org/10.1111/j.1151-2916.1984.tb19715.x.

[33] C. B. Liu, L. S. Yu, X. L. Jiang, Phase transition and grain growth kinetics of nanocrystalline 8% yttria stabilised zirconia powder, T. Nonferr. Metal. Soc. 21 (12) (2011) 3120-3128. https://doi.org/10.19476/j.ysxb.1004.0609.2011.12.021. (in Chinese)

[34] A. P. Singh, N. Kaur, A. Kumar, K. L. Singh, Preparation of Fully Cubic Calcium-Stabilised Zirconia With 10 mol% Calcium Oxide Dopant Concentration by Microwave Processing, J. Am. Ceram. Soc. 90 (3) (2010) 789-796. https://doi.org/10.1111/j.1551-2916.2006.01379.x.

[35] C. Li, M. J. Li, UV Raman spectroscopic study on the phase transformation of $ZrO_2$, $Y_2O_3$–$ZrO_2$ and $SO_4^{2-}$/$ZrO_2$, J. Raman Spectrosc. 33 (5) (2002) 301-308. https://doi.org/10.1002/jrs.863.

***Table captions***

Table 1 Chemical composition of zirconia raw material (wt. %).

***Figure captions***

Fig. 1 XRD results of CaO-PSZ.

Fig. 2 Schematic diagram of the microwave calcination equipment.

Fig. 3 The XRD results of the CaO-PSZ heated at 1100 ℃ show that the holding time is 1 h, 2 h, 3 h, and 4 h respectively.

Fig. 4 Corresponding XRD fitting diagram of (a) the as-received CaO-PSZ material, and microwave heating samples with a holding time of (b) 1 h, (c) 2 h, (d) 3 h, (e) 4 h at a temperature of 1100 ℃.

Fig. 5 Relative percentage of monoclinic and cubic phases in zirconia.

Fig. 6(a) Raman spectral analysis of CaO-PSZ; (b) Raman spectrum analysis of CaO-PSZ heated at 1100 ℃, holding time is 1 h, 2 h, 3 h and 4 h respectively.

Fig. 7 Corresponding Raman fitting diagram of (a) the as-received CaO-PSZ material, and microwave heating samples with a holding time of (b) 1 h, (c) 2 h, (d) 3 h, (e) 4 h at a temperature of 1100 ℃.

Fig. 8(a) FT-IR analysis of CaO-PSZ; (b) FT-IR analysis of CaO-PSZ heated at 1100 ℃, holding time of 1 h, 2 h, 3 h, and 4 h respectively.

Fig. 9 Scanning electron microscope image with a magnification of 10000 times: (a) heating products with 1100 °C holding time of 1 h; (b) heating products with 1100 °C holding time of 2 h; (c) heating products with 1100 °C holding time of 3 h; (d) heating products with 1100 °C holding time of 4 h.

Fig. 10 Stability rate of PSZ under different holding times.

Table 1 Chemical composition of zirconia raw material (wt. %).

| Composition | $ZrO_2$ | $Al_2O_3$ | $SiO_2$ | CaO | $Fe_2O_3$ | $TiO_2$ |
|---|---|---|---|---|---|---|
| Mass% | 94.85 | 0.4 | 0.4 | 4.0 | 0.15 | 0.2 |

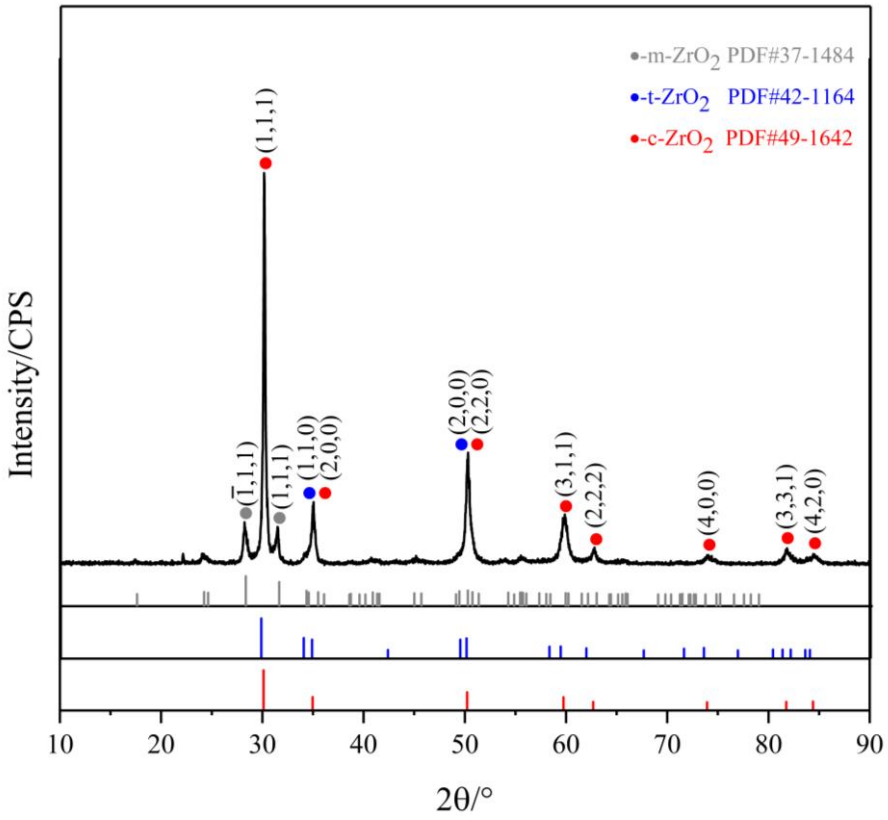


Fig. 1 XRD results of CaO-PSZ.

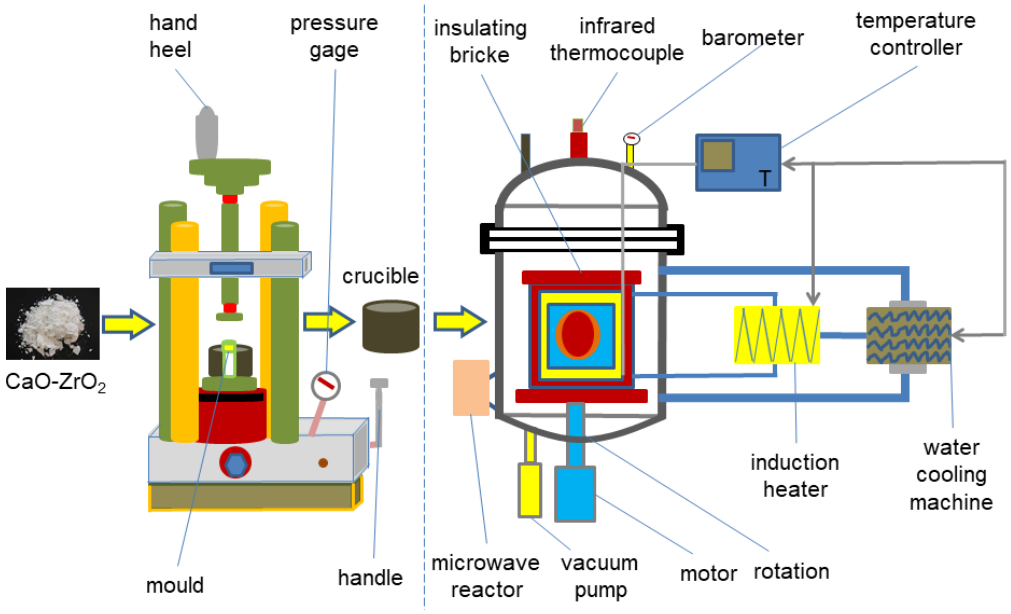


Fig. 2 Schematic diagram of the microwave calcination equipment.

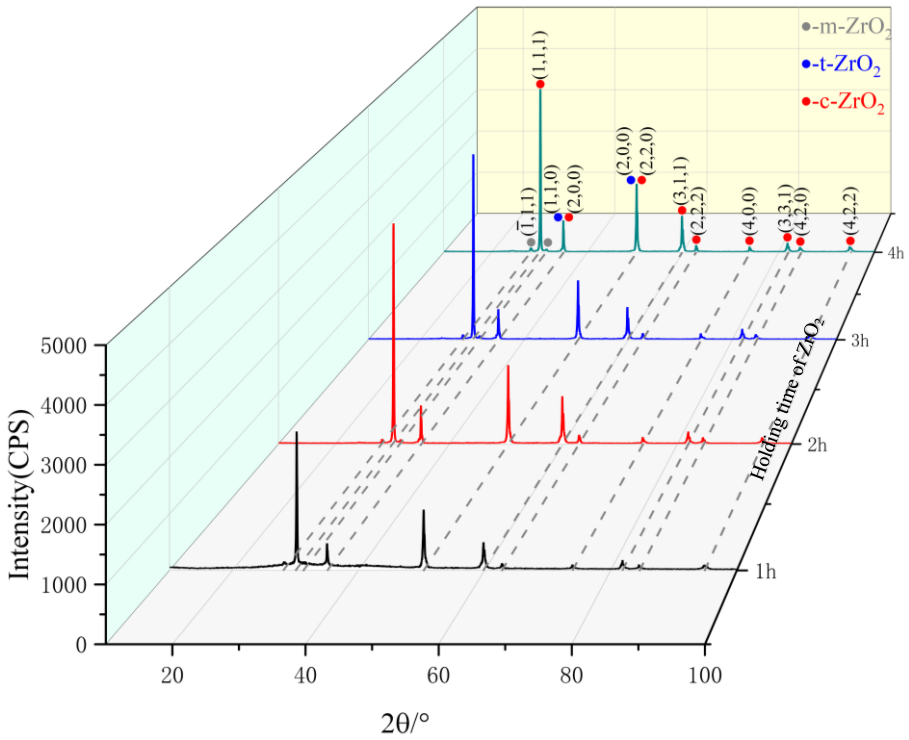


Fig. 3 The XRD results of the CaO-PSZ heated at 1100 ℃ show that the holding time is 1 h, 2 h, 3 h, and 4 h respectively.

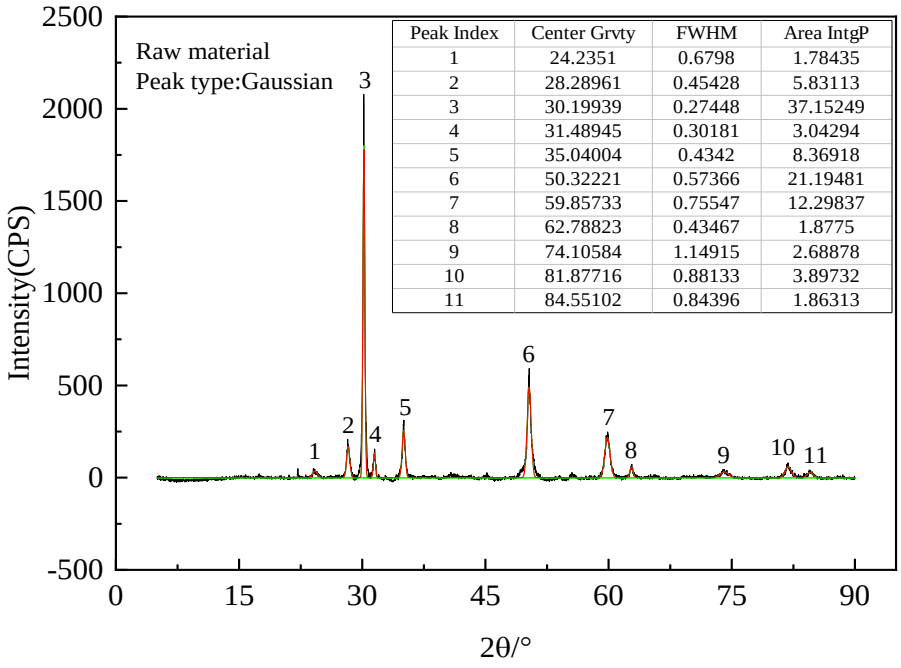


| Peak Index | Center Grvty | FWHM | Area IntgP |
|---|---|---|---|
| 1 | 24.2351 | 0.6798 | 1.78435 |
| 2 | 28.28961 | 0.45428 | 5.83113 |
| 3 | 30.19939 | 0.27448 | 37.15249 |
| 4 | 31.48945 | 0.30181 | 3.04294 |
| 5 | 35.04004 | 0.4342 | 8.36918 |
| 6 | 50.32221 | 0.57366 | 21.19481 |
| 7 | 59.85733 | 0.75547 | 12.29837 |
| 8 | 62.78823 | 0.43467 | 1.8775 |
| 9 | 74.10584 | 1.14915 | 2.68878 |
| 10 | 81.87716 | 0.88133 | 3.89732 |
| 11 | 84.55102 | 0.84396 | 1.86313 |

(a)

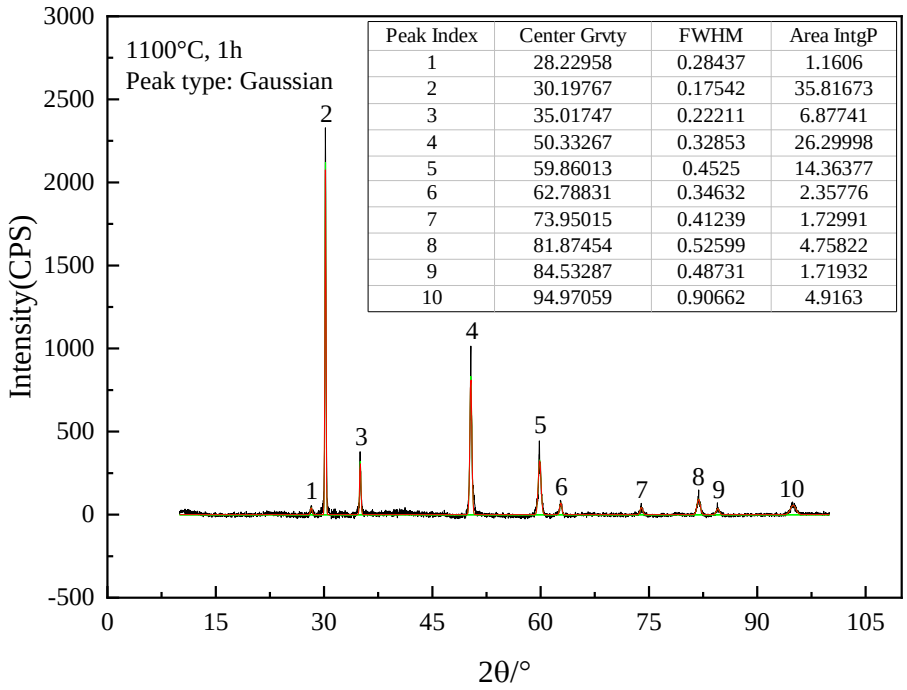


| Peak Index | Center Grvty | FWHM | Area IntgP |
|---|---|---|---|
| 1 | 28.22958 | 0.28437 | 1.1606 |
| 2 | 30.19767 | 0.17542 | 35.81673 |
| 3 | 35.01747 | 0.22211 | 6.87741 |
| 4 | 50.33267 | 0.32853 | 26.29998 |
| 5 | 59.86013 | 0.4525 | 14.36377 |
| 6 | 62.78831 | 0.34632 | 2.35776 |
| 7 | 73.95015 | 0.41239 | 1.72991 |
| 8 | 81.87454 | 0.52599 | 4.75822 |
| 9 | 84.53287 | 0.48731 | 1.71932 |
| 10 | 94.97059 | 0.90662 | 4.9163 |

(b)

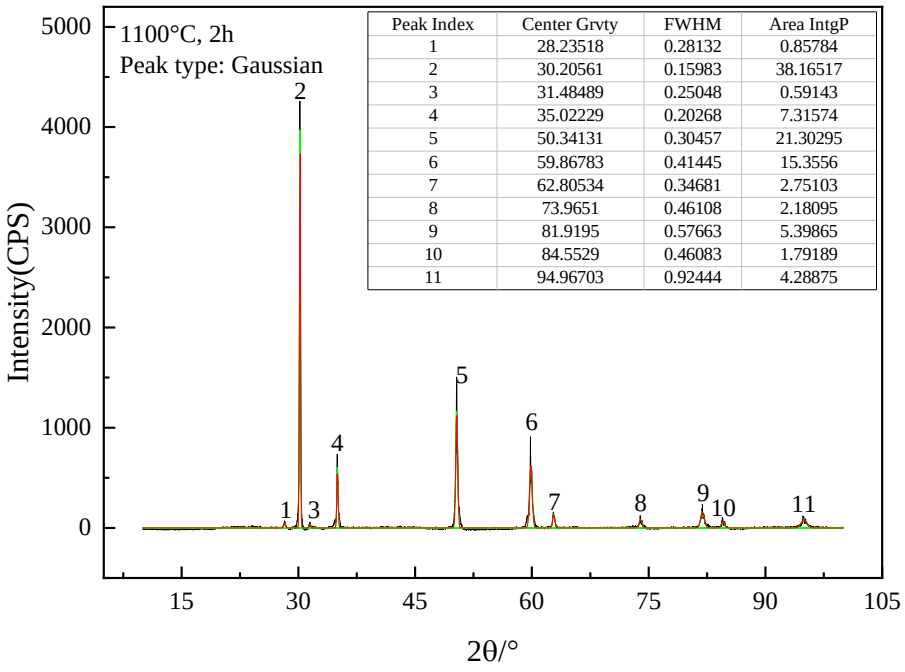


| Peak Index | Center Grvty | FWHM | Area IntgP |
|---|---|---|---|
| 1 | 28.23518 | 0.28132 | 0.85784 |
| 2 | 30.20561 | 0.15983 | 38.16517 |
| 3 | 31.48489 | 0.25048 | 0.59143 |
| 4 | 35.02229 | 0.20268 | 7.31574 |
| 5 | 50.34131 | 0.30457 | 21.30295 |
| 6 | 59.86783 | 0.41445 | 15.3556 |
| 7 | 62.80534 | 0.34681 | 2.75103 |
| 8 | 73.9651 | 0.46108 | 2.18095 |
| 9 | 81.9195 | 0.57663 | 5.39865 |
| 10 | 84.5529 | 0.46083 | 1.79189 |
| 11 | 94.96703 | 0.92444 | 4.28875 |

(c)

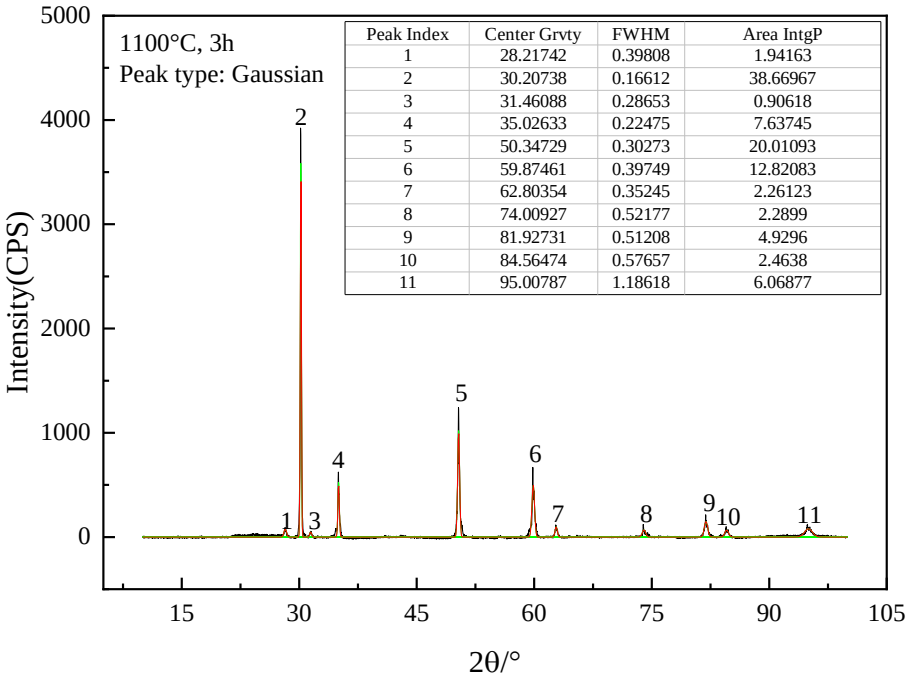


| Peak Index | Center Grvty | FWHM | Area IntgP |
|---|---|---|---|
| 1 | 28.21742 | 0.39808 | 1.94163 |
| 2 | 30.20738 | 0.16612 | 38.66967 |
| 3 | 31.46088 | 0.28653 | 0.90618 |
| 4 | 35.02633 | 0.22475 | 7.63745 |
| 5 | 50.34729 | 0.30273 | 20.01093 |
| 6 | 59.87461 | 0.39749 | 12.82083 |
| 7 | 62.80354 | 0.35245 | 2.26123 |
| 8 | 74.00927 | 0.52177 | 2.2899 |
| 9 | 81.92731 | 0.51208 | 4.9296 |
| 10 | 84.56474 | 0.57657 | 2.4638 |
| 11 | 95.00787 | 1.18618 | 6.06877 |

(d)

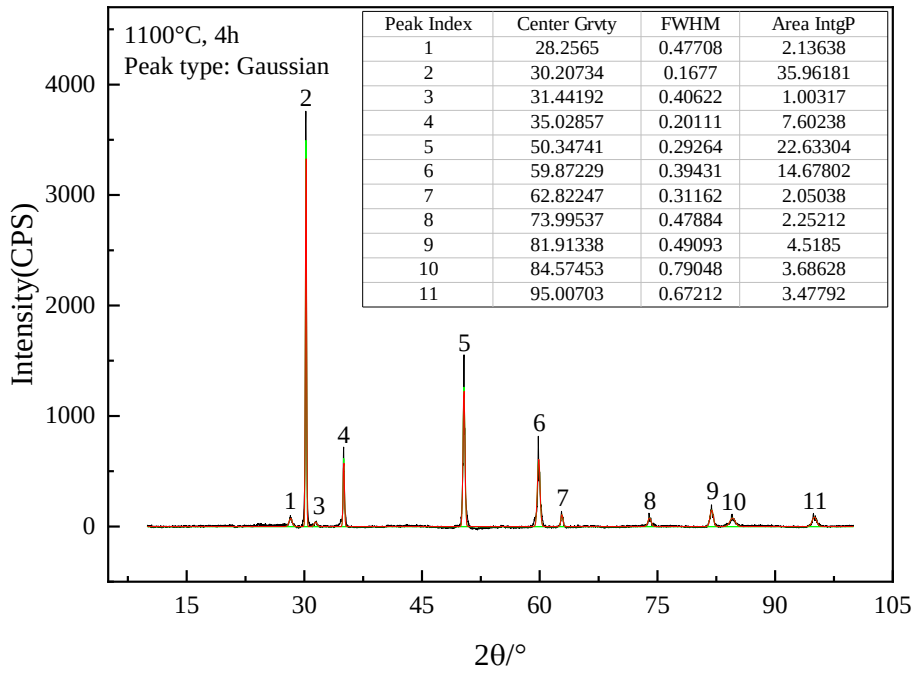


| Peak Index | Center Grvty | FWHM | Area IntgP |
|---|---|---|---|
| 1 | 28.2565 | 0.47708 | 2.13638 |
| 2 | 30.20734 | 0.1677 | 35.96181 |
| 3 | 31.44192 | 0.40622 | 1.00317 |
| 4 | 35.02857 | 0.20111 | 7.60238 |
| 5 | 50.34741 | 0.29264 | 22.63304 |
| 6 | 59.87229 | 0.39431 | 14.67802 |
| 7 | 62.82247 | 0.31162 | 2.05038 |
| 8 | 73.99537 | 0.47884 | 2.25212 |
| 9 | 81.91338 | 0.49093 | 4.5185 |
| 10 | 84.57453 | 0.79048 | 3.68628 |
| 11 | 95.00703 | 0.67212 | 3.47792 |

(e)

Fig. 4 Corresponding XRD fitting diagram of (a) the as-received CaO-PSZ material, and microwave heating samples with a holding time of (b) 1 h, (c) 2 h, (d) 3 h, (e) 4 h at a temperature of 1100 ℃.

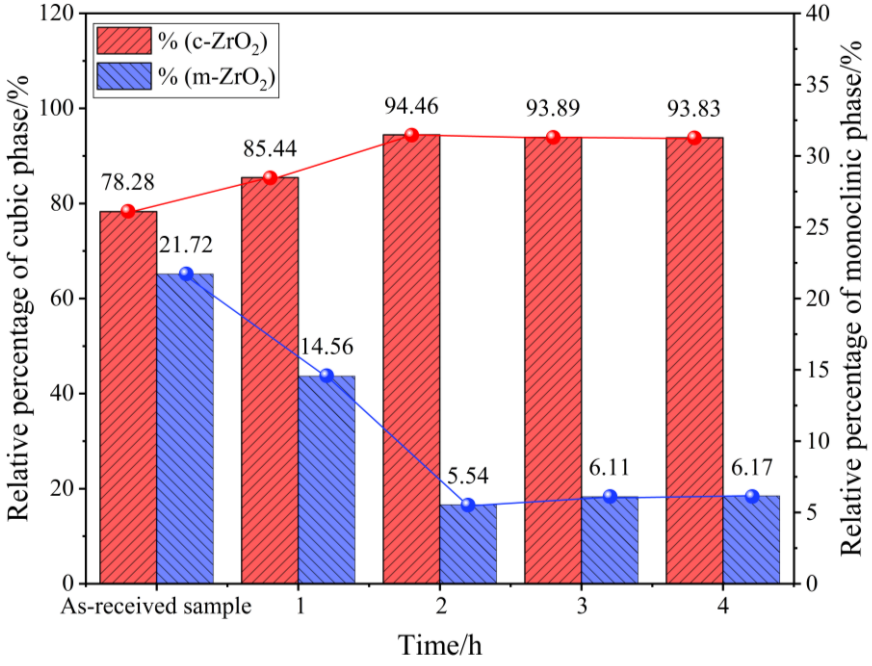


Fig. 5 Relative percentage of monoclinic and cubic phases in zirconia.

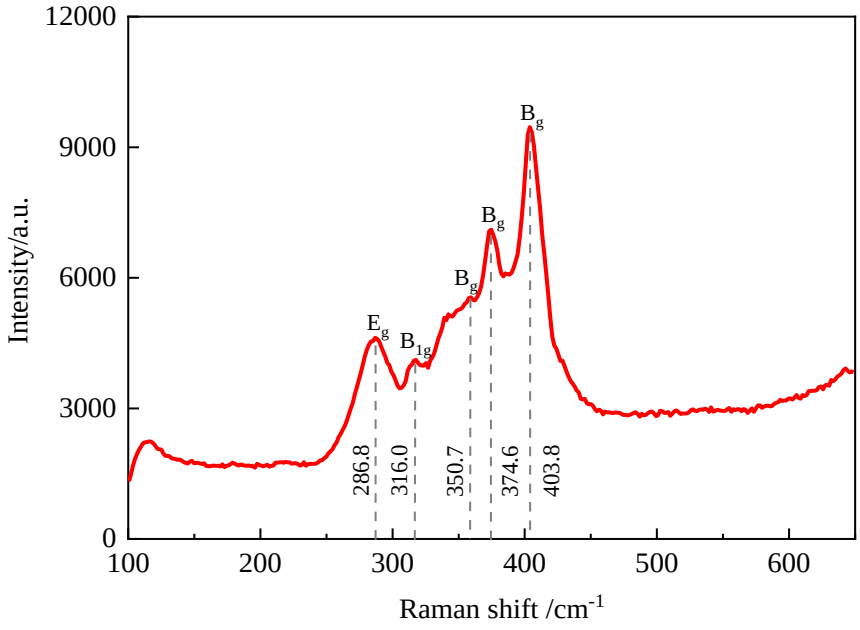
12000
9000
6000
3000
0
Intensity/a.u.
100
200
300
400
500
600
Raman shift /cm-1
Eg
B1g
Bg
Bg
Bg
286.8
316.0
350.7
374.6
403.8

(a)

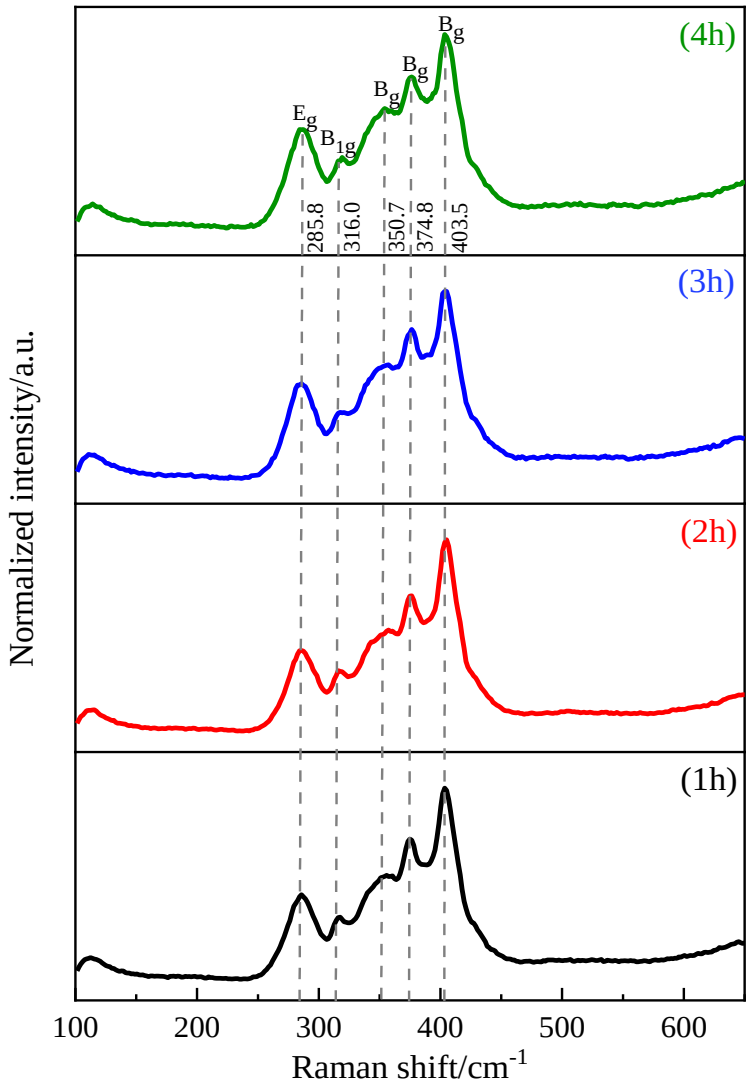


(b)

Fig. 6(a) Raman spectral analysis of CaO-PSZ; (b) Raman spectrum analysis of CaO-PSZ heated at 1100 ℃, holding time is 1 h, 2 h, 3 h and 4 h respectively.

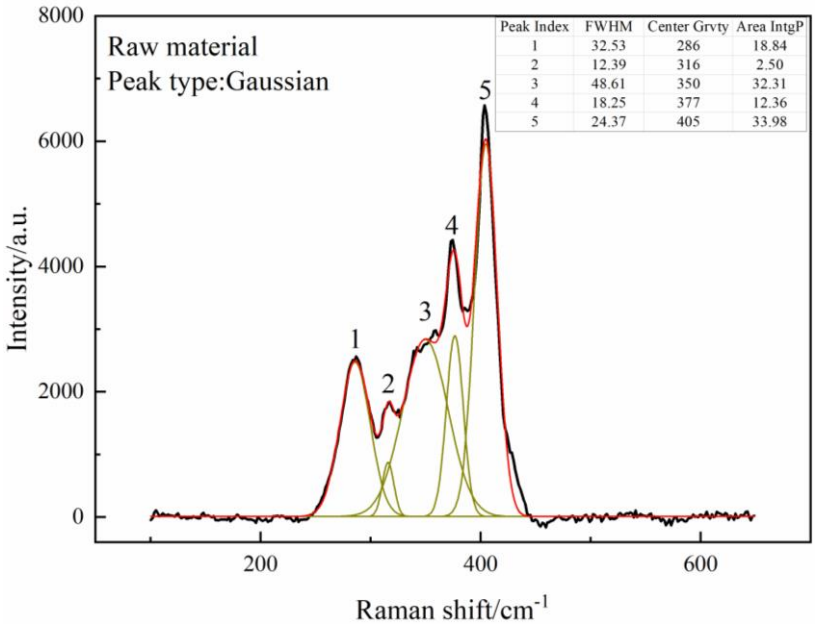
Raw material
Peak type:Gaussian
Peak Index FWHM Center Grvty Area IntgP
1 32.53 286 18.84
2 12.39 316 2.50
3 48.61 350 32.31
4 18.25 377 12.36
5 24.37 405 33.98
Intensity/a.u.
Raman shift/cm-1

(a)

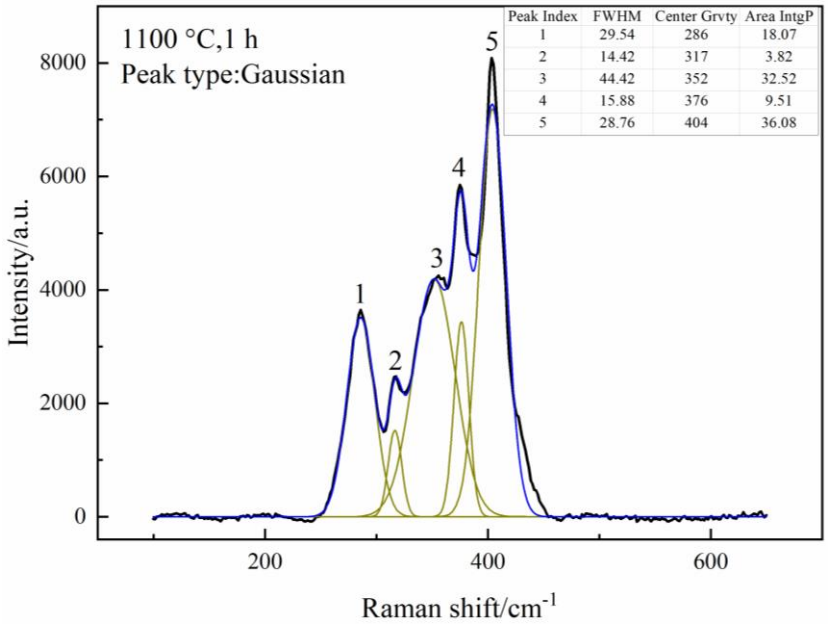
1100 °C,1 h
Peak type:Gaussian
Peak Index FWHM Center Grvty Area IntgP
1 29.54 286 18.07
2 14.42 317 3.82
3 44.42 352 32.52
4 15.88 376 9.51
5 28.76 404 36.08
Intensity/a.u.
Raman shift/cm-1

(b)

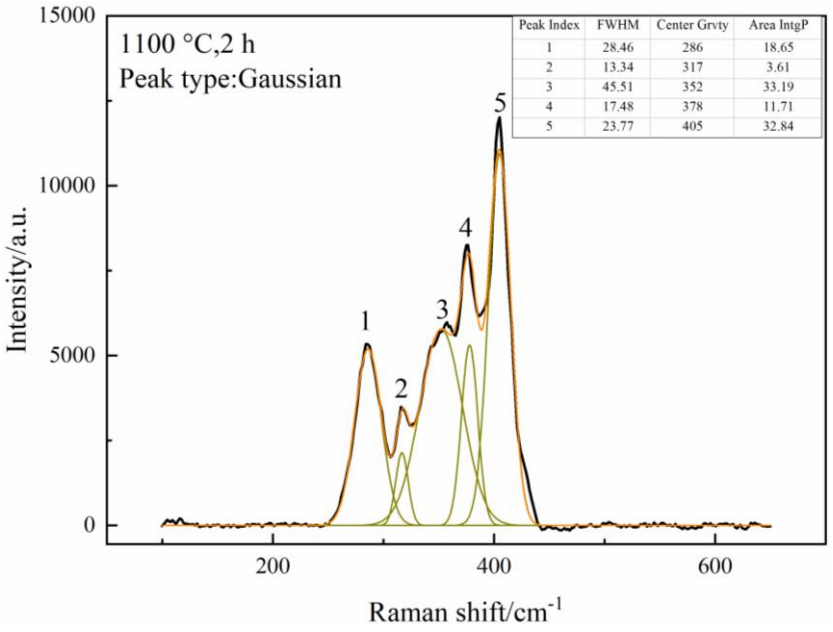
1100 °C,2 h
Peak type:Gaussian
Peak Index FWHM Center Grvty Area IntgP
1 28.46 286 18.65
2 13.34 317 3.61
3 45.51 352 33.19
4 17.48 378 11.71
5 23.77 405 32.84
Intensity/a.u.
Raman shift/cm-1

(c)

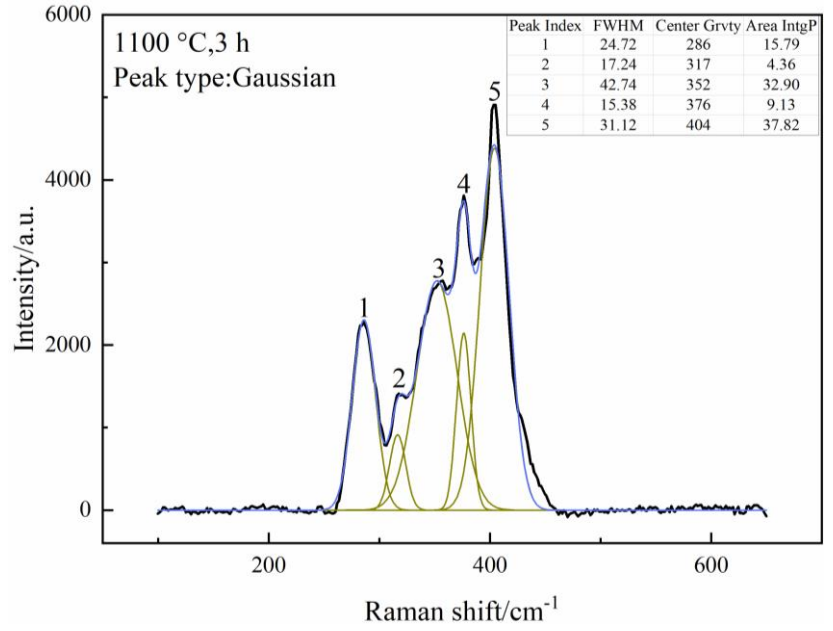
1100 °C,3 h
Peak type:Gaussian
Peak Index FWHM Center Grvty Area IntgP
1 24.72 286 15.79
2 17.24 317 4.36
3 42.74 352 32.90
4 15.38 376 9.13
5 31.12 404 37.82
Intensity/a.u.
Raman shift/cm-1

(d)

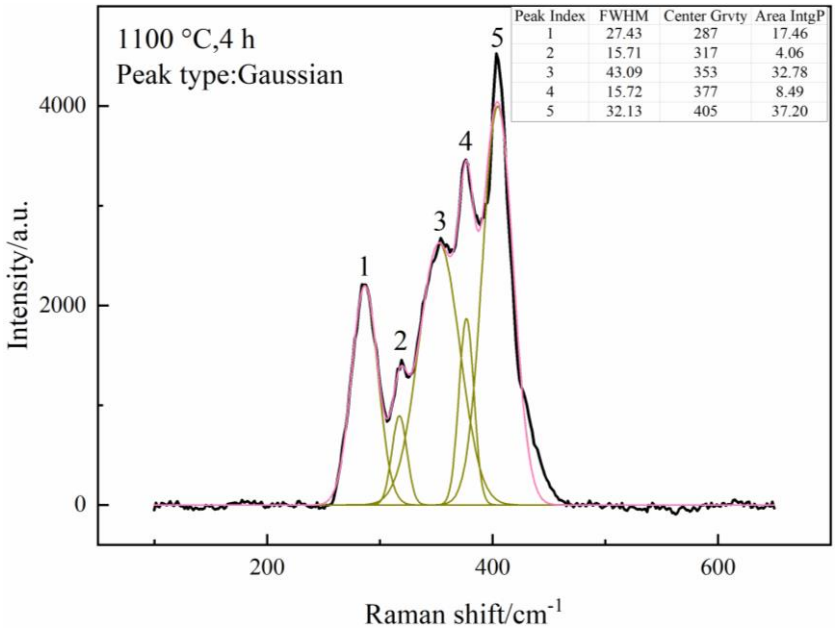


(e)

Fig. 7 Corresponding Raman fitting diagram of (a) the as-received CaO-PSZ material, and microwave heating samples with a holding time of (b) 1 h, (c) 2 h, (d) 3 h, (e) 4 h at a temperature of 1100 ℃.

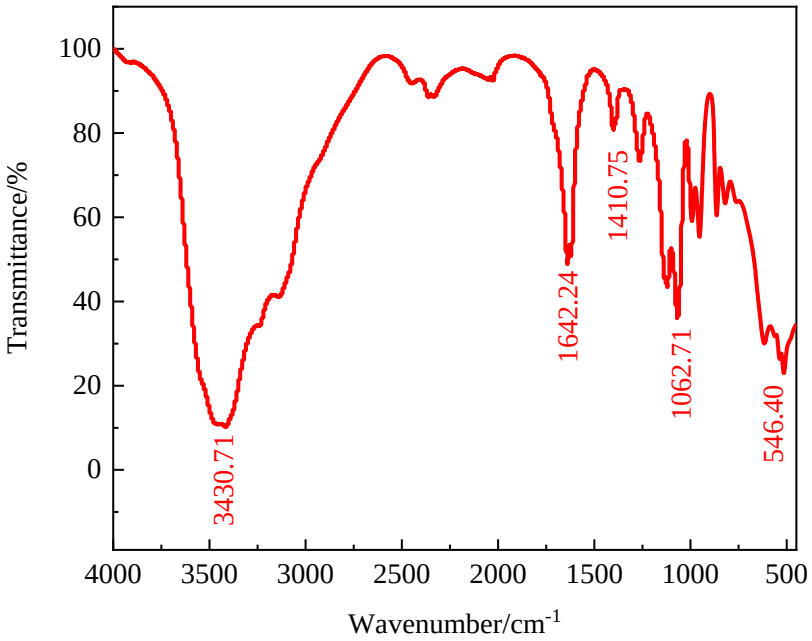
Transmittance/%
100
80
60
40
20
0
4000
3500
3000
2500
2000
1500
1000
500
Wavenumber/cm-1
3430.71
1642.24
1410.75
1062.71
546.40

(a)

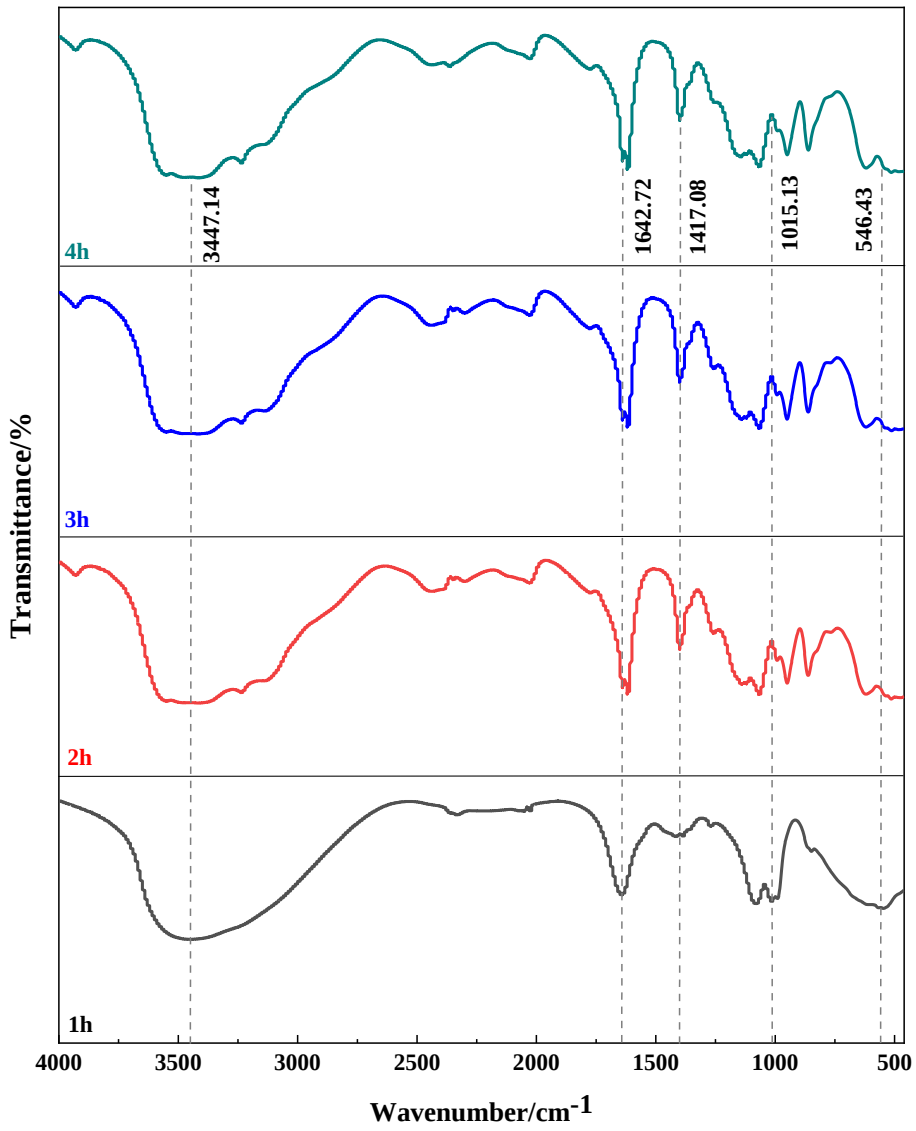


(b)

Fig. 8(a) FT-IR analysis of CaO-PSZ; (b) FT-IR analysis of CaO-PSZ heated at 1100 ℃, holding time of 1 h, 2 h, 3 h, and 4 h respectively.

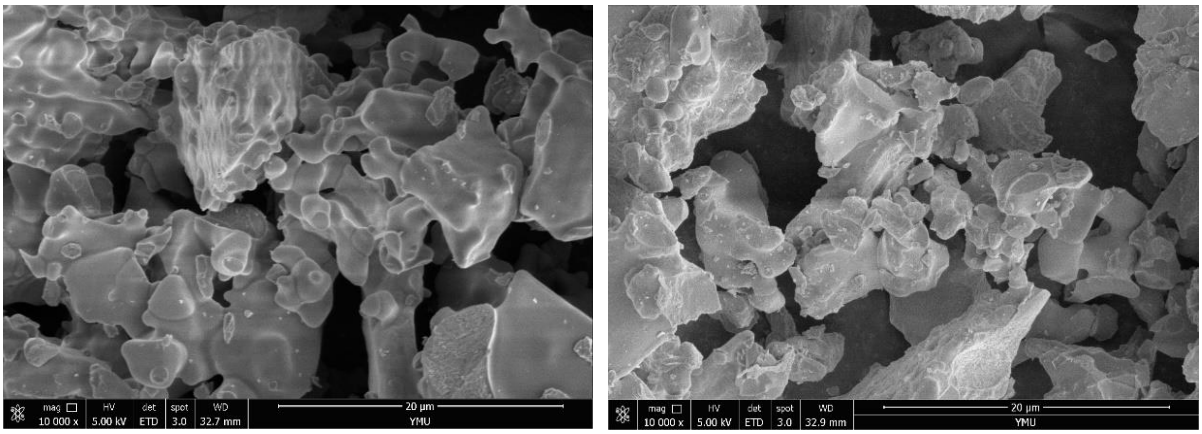


(a) (b)

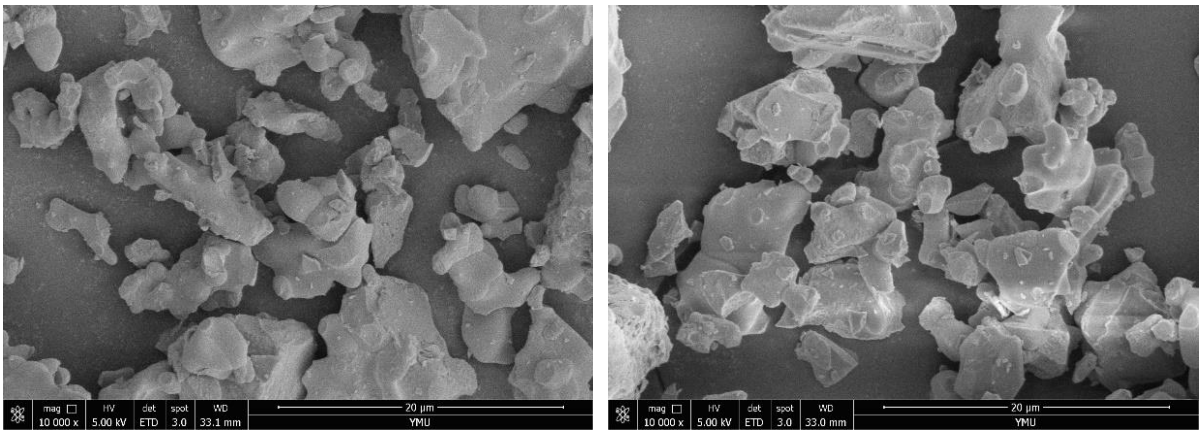


(c) (d)

Fig. 9 Scanning electron microscope image with a magnification of 10000 times: (a) heating products with 1100 °C holding time of 1 h; (b) heating products with 1100 °C holding time of 2 h; (c) heating products with 1100 °C holding time of 3 h; (d) heating products with 1100 °C holding time of 4 h.

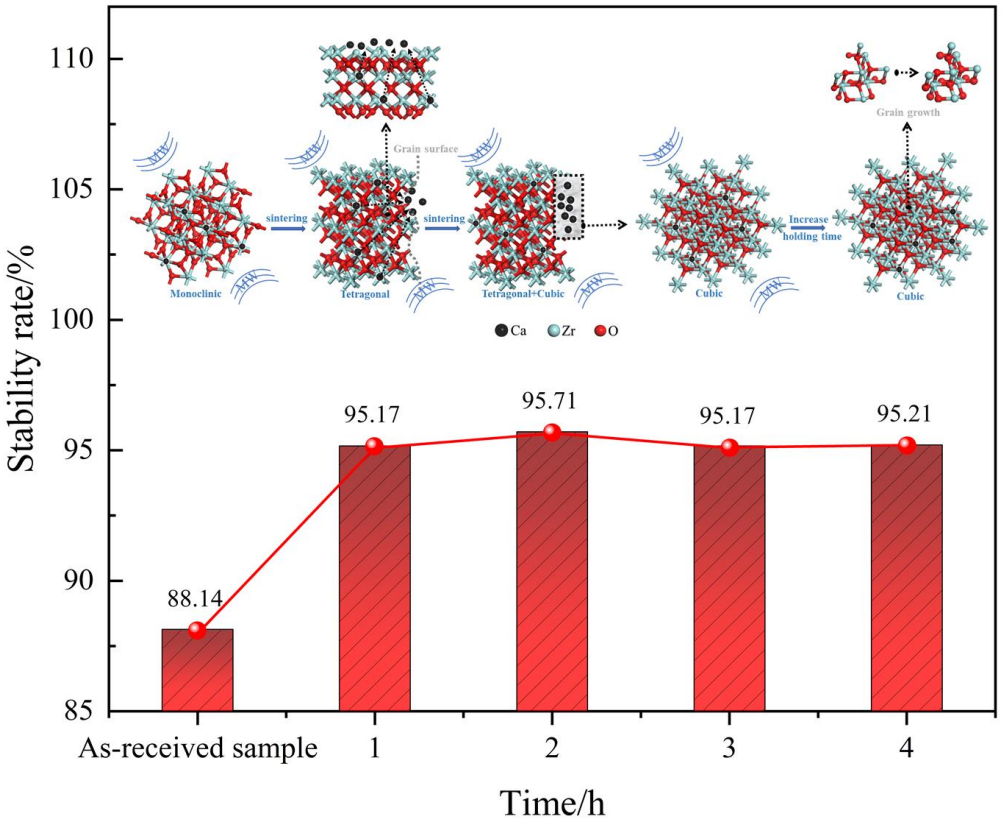


Fig. 10 Stability rate of PSZ under different holding times.